Tree Cover Discrimination in Panchromatic Aerial Imagery of Pinyon-Juniper Woodlands

Jesse Jacob Anderson and Neil S. Cobb

Abstract

Responding to an increasing interest in studying vegetation changes over time, we review current methods of processing black and white digital aerial photographs in order to classify tree cover in pinyon-juniper woodlands. Besides applying commonly used clustering and supervised maximum-likelihood methods, we have developed a new classifier, nearest edge thresholding, which is unsupervised and based on the principals of edge detection and density slicing. Comparison of the three methods' abilities to predict field values at plot scales of 100 m² to 900 m² shows this new method is better or comparable to others at all scales, can be easily applied to digital imagery, and has high correspondence with ground-truthed field values of tree cover.

Introduction

Studying long-term vegetation changes has become increasingly important in understanding the ecology of plant succession (Severson, 1986), effects of climate change on vegetation (Allen and Breshears, 1998), land-use impacts (Campbell, *et al.*, 1997), and as a predictive tool in ecosystem science and range management (Belsky, 1996). Unfortunately, past data on plant communities over large areas is sparse, difficult to combine with modern data, and often produced by personal testimonial evidence and repeated oblique photography that is largely qualitative and anecdotal (Creque, *et al.*, 1999).

Fine-scale (1:40000 and larger), black and white aerial photographs of many areas are widely available and can stretch back to the early 20th century, long before the advent of satellite-based remote sensing (Avery and Berlin, 1992). The detail and coverage of these images gives researchers the opportunity to retrieve high-resolution land-cover data in areas not historically sampled using conventional techniques. Additionally, matching historic and modern photographs can enable quantitative analysis of vegetative changes over time, attaching new importance and timeliness to the ability to process panchromatic aerial photographs in order to produce useful vegetation data.

Review of Aerial Photo Classification Techniques

Many studies in a number of fields have used aerial photographs as a tool to define historic or modern vegetation classes on the ground; of these, most have used manual interpretation to derive vegetation classes (Avery and Berlin, 1992; Fisher and Harris, 1999; Huebner, *et al.*, 1999), and few have utilized modern digital processing techniques (e.g., Mast, *et al.*, 1997; Carmel and Kadmon, 1999). However, we are not aware of any study that has conducted a comparative assessment of digital processing techniques for black and white aerial photographs. Digital processing techniques most often applied include image-level thresholding (Hutchinson, *et al.*, 2000) or supervised maximum-likelihood classification schemes (Kadmon and Harari-Kramer, 1999). Other digital techniques include analysis of zonal or image-level statistics (Shoshany, 2002; Avery and Berlin, 1992), and, more recently, pattern-recognition of tree-crowns (Uuttera, *et al.*, 1998; Haara and Nevalainen, 2002).

Most simple image classification techniques utilize imagery based on differences in grayscale levels between classes (Sonka, *et al.*, 1993). For instance, *thresholding* is simply choosing a cutoff value at which all darker values represent a separate output class than lighter values. To determine appropriate threshold values, a number of statistical techniques have been utilized or created to clearly differentiate classes. In some cases this thresholding value is based on user input, such as manual delineation of classes (Pitas, 2000).

More robust methods of image classification that are commonly used include unsupervised clustering algorithms and supervised methods, such as maximum-likelihood (or bayesian) classification. These methods rely on spectral separation of feature classes on an image level. K-means and ISODATA clustering, both commonly used, repeatedly iterate over arbitrary seed values and reassign pixel values to particular classes based on their closeness to these seed values, which are then recalculated to reflect mean class values; as the number of iterations increase, the mean class values gravitate towards natural breaks in the distribution of image pixels. Similarly, maximum-likelihood methods attempt to find class breaks within the spectral range of images. However, these breaks are based on *a priori* probabilities of classification into specific classes, usually based on user input of sample class values. These probabilities are used to assign pixel values to classes to minimize error in overall classification (Sonka, *et al.*, 1993; Pitas, 2000).

An important assumption of these classification schemes is that classes are spectrally independent over the input image; they therefore require relatively homogenous class values throughout. There are a number of ways to ensure this independence, each with potential to introduce further errors in classification. Schowengerdt (1997) suggested that outlying class values be removed from consideration for classification, either by deletion from the input image or, in supervised classification, from the input class signatures. Where possible, it is

Department of Biological Sciences, Merriam-Powell Center for Environmental Research, Northern Arizona University, Flagstaff AZ 86011 (Jesse.Anderson@nau.edu; Neil.Cobb@nau.edu).

important to preprocess images in such a way that increases separation of classes, using image normalization or other techniques. However, this has proven problematic, in some cases creating poorer final classification output than unaltered images (Carmel and Kadmon, 1998).

Other avenues for processing panchromatic digital images include fuzzy classification, which may assign multiple class values and associated probabilities to pixels (Zhang and Kirby, 1997; Brandtberg, 2002), pattern recognition of individual tree canopies (Larsen and Rudemo, 1998), and other techniques, some of which enhance existing classifiers (Baillard, *et al.*, 1998; Carmel and Kadmon, 1999). There are a number of reasons why these techniques have not been overly utilized in black and white image processing. First, these methods have been recently incorporated into GIS imagery analysis, often on multispectral satellite imagery. Because there is much less information in a single band image, application of such techniques to black and white photos may be difficult, or in some cases (for example, multispectral analysis) technically impossible. Second, panchromatic imagery is by its nature structurally simpler than multispectral images. The need for more complicated techniques may be low if available techniques are sufficient for, or can be adapted to, classification of panchromatic imagery with high accuracy.

Vegetation Change in Pinyon-Juniper

Pinyon-Juniper woodlands represent the third largest vegetation type in North America, and because they often encroach onto grasslands over time, they have come under close scrutiny for many years by ranchers and land managers (Severson, 1986; Belsky, 1996; Allen and Breshears, 1998; Campbell, *et al.*, 1999; and Creque, *et al.*, 1999). Because they are a historically dynamic system with broad ecological and economic importance, it is essential to improve our ability to quantify the spatio-temporal dynamics in tree cover in order to provide important ecological information needed for better management. For these reasons, we sought to develop methods that would most efficiently classify aerial photography into simple classes of tree and background features in order to extract quantitative data on woodland cover.

In approaching such a project, it is important to evaluate the applicability of current processing methods to such a system. Structural parameters of a forest type such as pinyon-juniper woodlands may constrain the usefulness of specific classification methods, especially when using historic aerial photographs. First, even on scales less than hectares, tree density, size, and species composition may vary greatly. On environmental gradients of several kilometers, vegetation often changes from sparsely forested grasslands to dense stands of mixed pinyon and juniper.

With these constraints in mind, we sought to apply image classification methods to recent aerial photographs of pinyon-juniper woodlands in order to determine which were best at classifying photographs into two groups: areas containing trees, and those containing background features such as grass, shrubs, and bare-ground. Initially, rather than focusing on developing new classification techniques, we applied density-slicing, ISODATA clustering, and supervised maximum-likelihood classification to apply to digital aerial photographs, since they were common in the literature and available in current software packages. However, visual inspection of the results of these techniques on a broad scale indicated that they may be insufficient in classifying trees at a range of densities and across local variation in image brightness, such as is present at different aspects of the same hill. With these issues in mind, we initiated a more thorough investigation of classification methods that culminated in the design of a new classification method, based on the techniques of thresholding, edge-detection, and nearest neighbor classification.

We present a new algorithm for classification of panchromatic aerial photographs into simple vegetation, in order to differentiate woody vegetation from grasses and bare ground and derive tree cover. The area of study is a large (167 km^2) area of pinyon-juniper woodland in northern Arizona, USA, stretching between grasslands at low elevations and ponderosa pine forest at high elevations. It contains a number of volcanic cinder cones, which represent the four cardinal aspects and a broad range of slopes. Our method processes each photo with an edge detection algorithm, and then uses values classified as tree edges to derive unique threshold values for each pixel's final classification. It has been implemented in both ERDAS© Imagine 8.4+ and ESRI ARCGIS© 8.x. To evaluate this methods' usefulness against other classifiers and real world scenarios, regression analysis is used to compare classifiers to ground-truthed field data across the entire range of tree density. Additionally, we are interested in knowing at what scale classification is most accurate. Therefore, each classifier's accuracy is evaluated at an incremental range of spatial scales from 100 m^2 to 900 m^2.

Methods

Algorithm Details

Our classification algorithm was designed to correctly quantify trees as small as one pixel wide (in this project, 1 meter resolution photos were used) in aerial photographs. It was also designed to work without extensive preprocessing of input digital photographs, including brightness transformations and/or normalization, smoothing, and convolution filtering. Upon detailed examination and testing of current classification schemes, we created a hybrid algorithm based on principles of thresholding, edge-based segmentation, and nearest-neighbor fuzzy classifiers.

Investigation of the results of image classification using ISODATA clustering and maximum-likelihood algorithms showed that misclassification was often attributable to different brightness values for the same vegetation class over large areas. As discussed, a central assumption of these and other basic image classifiers is that separate classes are represented by discrete differences between grayscale values. Overcoming this obstacle and finding unique class divisions present at different places throughout the image could prove to vastly improve classifier accuracy.

Starting with the most basic image segmentation technique, thresholding (or density-slicing), we used edge detection to find specific class separation values at any place in the digital image. As edge-detection works on the differences between pixels and not their absolute values (Sonka, *et al.*, 1993), deriving threshold values in this manner ensured local variation in image brightness would not reduce classification accuracy of the image.

Simple edge detection in imagery is straightforward; most edge detectors use simple convolution kernels to quantify the difference in grayscale values in cells neighboring a pixel. We chose a simple 3 × 3 orthogonal sobel kernel to calculate edge values for the input image. This method creates an arbitrary edge magnitude for any pixel; it does not explicitly define which pixels are edges. To accomplish this, we used a simple thresholding technique to define edges; edge values that were greater than one standard deviation above the mean edge value for the entire image were defined as edges.

With edge pixels defined, the actual values of these pixel values represented specific cutoff values for tree canopy throughout the image. In order to utilize these values to create a specific threshold value for each image pixel, we used a modified nearest neighbor algorithm as used in some fuzzy classification techniques (Carmel and Kadmon, 1999). Assuming that the closest edge values for a pixel most accurately described

the tree to background threshold value for that area, aggregating nearby edge values could produce a unique threshold cutoff value for any pixel. We first calculated the distance to an edge cell for every pixel in the image. We then used these distance values to determine the maximum distance to the nearest edge within the image. In order to maximize efficiency, we used the mean distance to an edge for all pixels plus three standard deviations of that mean instead of the absolute maximum (Ott, 1993).

With both edges and the distance to edges defined for the input image, a specific threshold value could be created for any pixel. This was accomplished by calculating the mean value of all edge pixels within the window specified by the maximum distance value derived above for every pixel. This produced a grid of specific threshold values for each input image. The input image was then classified using these values: if a pixel was darker than its overlaying threshold value, it was classified as tree area; otherwise, it was classified as some other background feature. This algorithm was implemented in ERDAS© Imagine 8.4 using the spatial modeler tools and was also written in ARC© macro language for use in ARCGIS© Workstation 8.2.

Image Processing

We obtained digital orthophoto quadrangles with one meter resolution created by the USGS (1 meter pixel size) from aerial photographs taken between July 1997 and October 1998 for use as test images (Figure 1). The specific requirements of such imagery are that the sun angle is thirty degrees or higher to reduce potential shadow effects on the ground, cloud cover must be absent, and atmospheric haze must be minimal.

Shading effects are a concern in analyzing air photos, including shading caused by the position of the sun and large topographic features such as hills and mountains (Shoshany, 2002). Because our method determined threshold for tree to non-tree values on a local level, large features were not a problem. Additionally, in the area studied, the dominant species were very rarely over four meters tall. This reduced the influence of shading effects from individual trees in determining percent cover.

Accuracy Assessment

To assess accuracy of the tree-detection algorithm, we compared derived percent cover values from 1997 aerial photographs to ground-truthed for field percent cover values in the
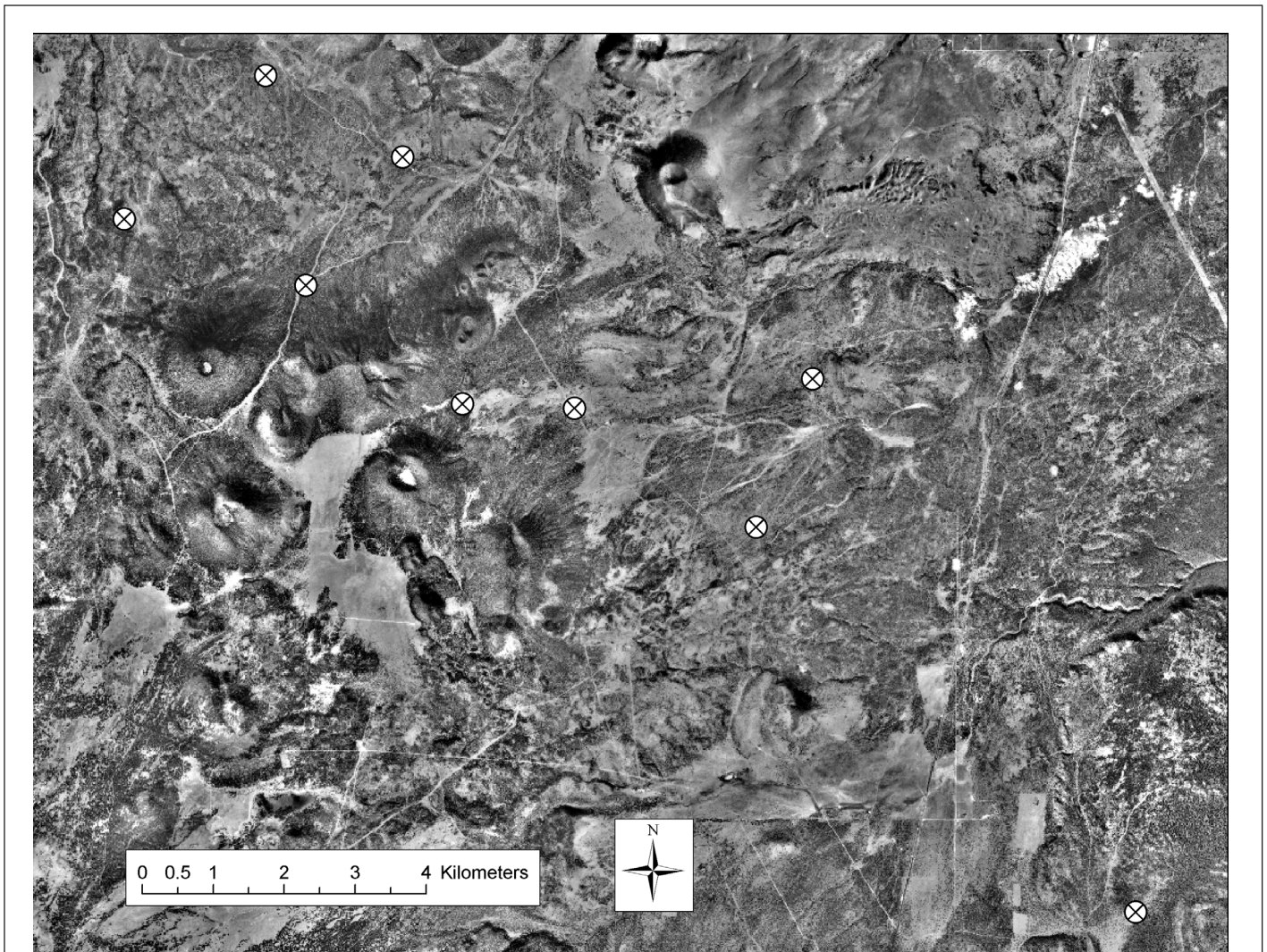
Figure 1. The marked places indicate where transects were erected for use in ground-truthing classification methods. Each transect was a 30 by 30 m square separated into individual 10 by 10 m sections. The total area covered by the map below is approximately 160 km².

same areas, recorded between 1998 and 2003. Field data was obtained for nine transects that were randomly selected in the area covered by the photographs (Figure 1) representing a range of woodland densities and surface topography. Each transect consisted of nine 100 m² sections in a 3 × 3 square. In each 100 m² section, the four edges were permanently marked with rebar and geographic positions recorded using a differentially-corrected Trimble Geoexplorer 3®. Tree canopy area of pinyon (*Pinus edulis*) and juniper (*Juniperus monosperma*) was determined by randomly selecting a point at the base of the canopy and estimating the average canopy extent along a decimeter-incremented pole. We then placed the pole perpendicular to the initial position and estimated average canopy diameter to the nearest decimeter and calculated the average of the two values to obtain tree canopy diameter. We presumed each tree was a circle and calculated canopy area. Two or more tree canopies that overlapped were calculated as a single area of canopy coverage. Summing these measurements provided a single value of canopy cover per section, combining pinyon and juniper.

These images were processed in ARCGIS© 8.2 using the algorithm detailed above (Figure 2). Once the images were reclassified into tree versus non-tree pixels, we derived a percent tree cover value for each 100 m² section. Additionally, we processed each image using an unsupervised ISODATA clustering algorithm with a 0.950 convergence threshold and a supervised, maximum-likelihood classification (Figure 2). We manipulated parameters of both methods in order to produce the best possible results for each, based both on information from the literature (Schowengerdt, 1997) and from trial runs of each classifier. The final input parameters for the clustering classification was an ISODATA algorithm with four output classes, a 95% convergence threshold, and initial seed values initialized from image statistics. For the maximum-likelihood classification, we created three pairs of input signatures for tree and background at low, medium, and high tree densities, each comprised of up to ten individual areas.

We used regression analyses to test the accuracy of each classification method against field data and across increasing study plot size. Because of the nested nature of our field study plots, we used a modified bootstrap method (Efron, 1993) to resample data, in order to reduce autocorrelation in the data values yet still ensure all field data was fully utilized. The outline of these methods are as follows:

1. Select one 10 × 10 meter section at random out of each 30 × 30 meter study plot, for a total of nine 10 × 10 meter sections, one for each of the nine study plots.
2. Calculate the regression equation and R^2 correlation coefficient for these nine points.
3. Replace these nine values many times, each time calculating mean regression coefficients for all samples.
4. Increase the scale of the analysis from 100 m² to 200 m² and repeat steps 1–3; increase repeatedly in 100 m² until the entire 30 × 30 meter (900 m²) plot is sampled.

In order to ensure that the true correlation between ground-truthed and photo-derived values was determined and all possible data combinations were used, we ran this for each classifier through 10,000 iterations. Once we derived tables of slope and correlation for all three methods at all scales, we compared these values among three methods to determine which best-predicted field data values.

Results

We analyzed the nearest edge thresholding method for accuracy at increasing scale and found it performed well at a plot size of even 100 m². The average R^2 value for 10,000 regressions made of randomly selected points, one from each of the
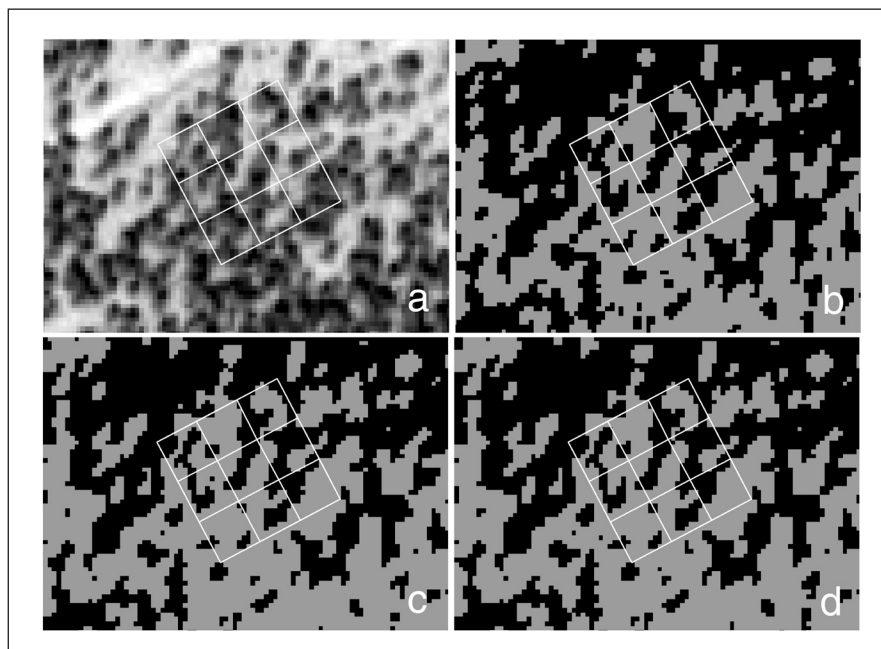
Figure 2. Examples of the three classification techniques detecting tree canopies over a small portion of a digital orthophoto. The outlined boxes are the 30 by 30 m transects showing the divisions into 10 by 10 m sections. The first picture (a) is the aerial image denoting pinyon and juniper canopies, the other images are canopy designations using classifications based on (b) nearest edge threshold, (c) maximum-likelihood and (d) ISODATA clustering. Lighter areas represent trees, and darker values are non-tree pixels.

TABLE 1. COMPARISON OF THREE CLASSIFICATION TECHNIQUES PREDICTING WOODLAND COVER ACROSS A RANGE OF SPATIAL SCALES. THE REGRESSION COEFFICIENT VALUES FOR THE NEAREST EDGE THRESHOLDING, MAXIMUM-LIKELIHOOD, AND ISODATA CLUSTERING CLASSIFIERS FROM 100 M² TO 900 M² SHOWS THAT NEAREST EDGE THRESHOLDING IS THE BEST OVERALL PREDICTOR OF PINYON-JUNIPER WOODLAND AREA. THE MAXIMUM LIKELIHOOD METHOD IS INTERMEDIATE IN PREDICTING WOODLAND COVER, AND ISODATA CLUSTERING PROVIDED THE LOWEST QUALITY PREDICTION OF VARIATION IN WOODLAND COVER.

Classification Method	Regression Statistics	Spatial Scale								
		$100 \ m^2$	$200 \ m^2$	$300 \ m^2$	$400 \ m^2$	$500 \ m^2$	$600 \ m^2$	$700 \ m^2$	$800 \ m^2$	$900 \ m^2$
Nearest Edge Thresholding	R^2	0.823	0.906	0.935	0.953	0.965	0.972	0.977	0.981	0.983
	Slope	0.944	1.049	1.112	1.134	1.143	1.154	1.159	1.168	1.175
	Y-intercept	0.050	0.050	0.043	0.031	0.019	0.003	−0.012	−0.030	−0.049
Maximum Likelihood	R^2	0.762	0.859	0.893	0.914	0.928	0.938	0.945	0.950	0.954
	Slope	0.635	0.699	0.739	0.751	0.756	0.761	0.764	0.770	0.775
	Y-intercept	0.041	0.050	0.056	0.061	0.064	0.067	0.070	0.069	0.068
ISODATA Clustering	R^2	0.736	0.821	0.861	0.881	0.893	0.900	0.905	0.908	0.911
	Slope	0.970	1.081	1.155	1.182	1.193	1.204	1.209	1.216	1.223
	Y-intercept	0.161	0.264	0.351	0.439	0.529	0.618	0.707	0.795	0.881

nine transects, was 0.823, with a slope of 0.955 and a y-intercept of 0.050 (Table 1). Correlation coefficient values increased steadily up to a scale of 900 m², where the R^2 was 0.983, the slope 1.175, and the y-intercept −0.049 (Table 1).

Comparison of different classification methods showed that nearest edge thresholding was better or comparable to the other two methods in predicting ground-truthed values of percent cover in all measurements (Table 1, Figure 3). At all scales, nearest edge thresholding values accounted for a greater amount of variation in field data than the clustering and maximum-likelihood methods (Figure 3). Additionally, the slope and y-intercept values were consistently close to one and zero, respectively, indicating a one-to-one relationship between field and photo-derived values (Table 1).

A repeated measures ANOVA was performed for each of the three classification schemes at scales of 100 m² and 900 m², showing that nearest edge thresholding performed better than the other methods in these cases. At 100 m², nearest edge thresholding values were non-significantly different from field values, with a p-value of 0.053; the values for clustering and maximum-likelihood method were both different from field

values with $p = 0.017$. At 900 m², both maximum-likelihood and nearest edge thresholding values were not significantly different from field values, with p-values of 0.081, and 0.099, respectively; clustering values were significantly different with $p = 0.005$.

Discussion

Results from comparison of field data and photo-derived values for all classifiers showed that they performed satisfactorily at a variety of scales. Nearest-edge thresholding was a better predictor of field determined canopy areas than maximum-likelihood or ISODATA clustering, as shown by the repeated measures ANOVA. Additionally, nearest edge thresholding may be more appropriate in most cases because it is efficient, can be run on large data sets unsupervised, and is comparable to or out-performs other classifiers in all cases.

Examination of slope and y-intercept values for the regression results indicates to what extent each method over and underestimates field values at any scale. Since values for these coefficients changed in a constant direction for each classifier at increasing scale, an investigation of the extreme scales (100 m² and 900 m²) shows the range of variation in slope and y-intercept (Table 1). Slope values for nearest edge thresholding varied from 0.944 at the 100 m² scale to 1.175 at 900 m². These values, coupled with y-intercept values ranging from 0.050 to −0.049 show that nearest edge thresholding may overestimate low density percent cover and underestimate high density percent cover at small scales, and do the opposite at large scales. However, these values are consistently close to 1 and 0, respectively, making these errors fairly small. The coupled slope and intercept values for the other methods prove to be more problematic. While clustering slope values are close to 1 at small scales, the y-intercept is 0.161 at a scale of 100 m² and 0.881 at a scale of 900 m², values which introduce significant errors in field data correspondence. Likewise, maximum-likelihood intercept values range from 0.041 to 0.070, which are comparable to nearest edge thresholding, but slope values range from 0.635 to 0.775, which all underestimate percent cover at high density.

We compared classifiers and accuracy across plot scale in order to determine at what plot size classifiers performed best. Of high importance to projects that involve aerial photo classification is the size that must be used for field plots to guarantee high correspondence with classified values. While there is no definite cutoff point for high classification accuracy, researchers may choose study-specific cutoff values for regression coefficients which data must meet. For instance, if an R^2 of 0.90 and higher, a slope within 0.25 of 1, and a y-intercept within 0.25 of 0 is required, the appropriate scale would be
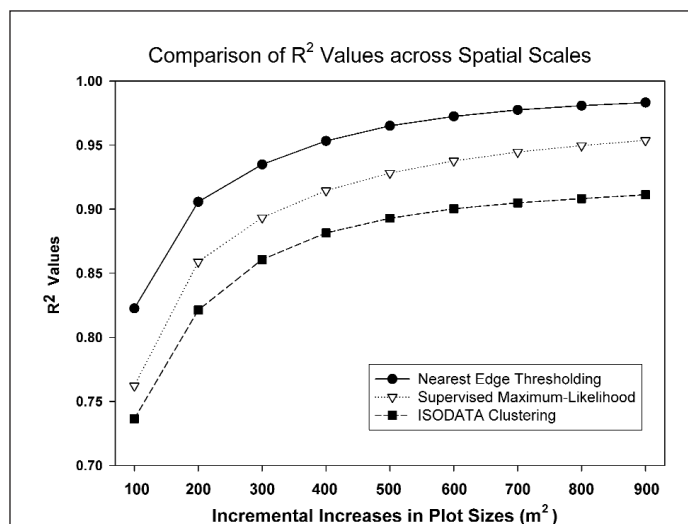
Figure 3. Correlation coefficient (R^2) values for the nearest edge thresholding, maximum-likelihood, and ISODATA clustering methods at increasing scales of 100 m² intervals. Nearest edge thresholding was the best predictor at all scales.

200 m^2 plot size for nearest edge thresholding, 400 m^2 for maximum-likelihood classification, and 800 m^2 for ISODATA clustering.

Overall, nearest edge thresholding outperformed ISODATA clustering and to a lesser degree, maximum-likelihood classification. We suggest that nearest edge thresholding is a more appropriate method to use in many situations. Since it is an unsupervised classifier that can be used *out of the box* with no prior knowledge of photo characteristics or processing parameters, it can be much more easily applied to digital photographs by researchers who may not have a strong background in image processing, particularly those interested in combining historic and modern aerial photographs into quantitative data sets for use in ecological modeling. Because it was developed for panchromatic photos, it is more specific and useful in extracting usable vegetation coverage from historical aerial photos than many recently developed methods focusing on multispectral aerial and satellite imagery. With the current interest in utilizing historic aerial photographs to detect vegetative change across decades, it may prove of great use in such areas as landscape ecology, land management, urban planning, and climate-change research.

Acknowledgments

References

Allen, C.D., and D.D. Breshears, 1998. Drought-induced shift of a forest-woodland ecotone: Rapid landscape response to climate variation, *Proceedings of the National Academy of Sciences of the United States of America*, 95:14839–42.

Avery, T.E., and G.L. Berlin, 1992. *Fundamentals of Remote Sensing and Airphoto Interpretation*, 5th edition, Prentice Hall, Upper Saddle River, New Jersey, 472 p.

Baillard, C., O. Dissard, O. Jamet, and H. Maître, 1998. Extraction and textural characterization of above-ground areas from aerial stereo pairs: A quality assessment, *ISPRS Journal of Photogrammetry and Remote Sensing*, 53:130–141.

Belsky, A.J., 1996. Viewpoint: Western juniper expansion: Is it a threat to arid northwestern ecosystems?, *Journal of Range Management*, 49:53–59.

Brandtberg, T., 2002. Individual tree-based species classification in high spatial resolution aerial images of forests using fuzzy sets, *Fuzzy Sets and Systems*, 132:371–387.

Campbell, R.B. Jr., S.B. Monsen, and R. Stevens, 1999. Ecology and management of pinyon-juniper communities within the Interior West: Overview of the "Ecological Restoration" session of the symposium (Monsen S.B. and R. Stevens, editors), Proceedings: Ecology and management of pinyon-juniper communities within the Interior West, 15–18 September, 1997, Provo, UT, (Rocky Mountain Research Station, Provo, Utah):271–277.

Carmel, Y., and R. Kadmon, 1998. Computerized classification of Mediterranean vegetation using panchromatic aerial photographs, *Journal of Vegetation Science*, 9:445–454.

Carmel, Y., and R. Kadmon, 1999. Effects of grazing and topography on long-term vegetation changes in a Mediterranean ecosystem in Israel, *Plant Ecology*, 145:243–254.

Creque, J.A., N.E. West, and J.P. Dobrowolski, 1999. Methods in historical ecology: A case study of Tintic Valley, Utah (Monsen, S.B., and R. Stevens, editors), Proceedings: Ecology and management of pinyon-juniper communities within the Interior West, 15–18 September, 1997, Provo, UT, (Rocky Mountain Research Station, Provo, Utah):121–133.

Efron, B., 1993. *An Introduction to the Bootstap*, 1st edition, Chapman and Hall, New York, New York.

Fisher, A.M., and S.J. Harris, 1999. The dynamics of tree cover change in a rural Austrailian landscape, *Landscape and Urban Planning*, 45:193–207.

Haara, A., and S. Nevalainen, 2002. Detection of dead or defoliated spruces using digital aerial data, *Forest Ecology and Management*, 160:97–107.

Huebner, C.D., J.L. Vankat, and W.H. Renwick, 1999. Change in the vegetation mosaic of central Arizona USA between 1940 and 1989, *Plant Ecology*, 144:83–91.

Hutchinson, C.F., J.D. Unruh, and C.J. Bahre, 2000. Land use vs. climate as causes of vegetation change: A study in SE Arizona, *Global Environmental Change*, 10:47–55.

Kadmon, R., and R. Harari-Kremer, 1999. Studying long-term vegetation dynamics using digital processing of historical aerial photographs, *Remote Sensing of Environment*, 68:164–176.

Larsen, M., and M. Rudemo, 1998. Optimizing templates for finding trees in aerial photographs, *Pattern Recognition Letters*, 19: 1153–1162.

Mast, J.N., T.T. Veblen, and M.E. Hodgson, 1997. Tree invasion within a pine/grassland ecotone: An approach with historic aerial photography and GIS modeling, *Forest Ecology and Management*, 93: 181–194.

Ott, R.L., 1993. *An Introduction to Statistical Methods and Data Analysis*, 4th edition, Duxbury Press, Belmont, California.

Pitas, I., 2000. *Digital Image Processing Algorithms and Applications*, 1st edition, John Wiley and Sons, New York, New York.

Pouliot, D.A., D.J. King, F.W. Bell, and D.G. Pitt, 2002. Automated tree crown detection and delineation in high-resolution digital camera imagery of coniferous forest regeneration, *Remote Sensing of Environment*, 82:322–334.

Schowengerdt, R.A., 1997. *Remote Sensing Models and Methods for Image Processing*, 2nd edition, Academic Press, San Diego, California.

Sebego, R.J.G., and W. Arnberg, 2002. Interpretation of mopane woodlands using air photos with implications on satellite image classification, *International Journal of Applied Earth Observation and Geoinformation*, 4:119–135.

Severson, K.E., 1986. Woody plant reestablishment in modified pinyon-juniper woodland, New Mexico, *Journal of Range Management*, 39:438–442.

Shoshany, M., 2002. Landscape fragmentation and soil cover changes on south- and north-facing slopes during ecosystems recovery: An analysis from multi-date air photographs, *Geomorphology*, 45(1-2):3–20.

Sonka, M., V. Hlavac, and R. Boylem, 1993. *Image Processing, Analysis, and Ma*chine *Vision*, 1st edition, Chapman & Hall, London, UK.

Uuttera, J., A. Haara, T. Tokola, and M. Maltamo, 1998. Determination of spatial distribution of trees from digital aerial photographs, *Forest Ecology and Management*, 110:275–282.

Zhang, J., and R.P. Kirby, 1997. An evaluation of fuzzy approaches to mapping land cover from aerial photographs, *ISPRS Journal of Photogrammetry and Remote Sensing*, 52:193–201.